

## RESEARCH ARTICLE

# The Art of Substrate-Integrated-Waveguide Power Dividers

**FARAH BILAWAL**<sup>ID</sup>, (Member, IEEE), **FATEMEH BABAEIAN**<sup>ID</sup>, (Member, IEEE),  
**KIM TUYEN TRINH**<sup>ID</sup>, (Member, IEEE), AND **NEMAI CHANDRA KARMAKAR**<sup>ID</sup>, (Senior Member, IEEE)

Department of Electrical and Computer Systems Engineering, Monash University, Melbourne, VIC 3800, Australia

Corresponding author: Farah Bilawal (farah.bilawal@monash.edu)

This work was supported by the Australian Research Council (ARC) through Passive Airborne Radiometer for High-Resolution Soil Moisture Monitoring under Grant DP160104233.

**ABSTRACT** Substrate-integrated-waveguide (SIW) technology can eliminate the limitations associated with conventional rectangular waveguides, i.e., bulky structures and production complexity at higher frequencies. Moreover, SIW technology replaces microstrip structures eliminating the drawback of excessive radiation leakage at higher frequencies. SIW power dividers are key elements in SIW antenna array synthesis. A SIW power divider's design procedures are more complicated than conventional microstrip power dividers. However, no comprehensive review with design guidelines of substrate-integrated-waveguide (SIW) power dividers has been reported. In this paper, different types of SIW power dividers based on their configurations, functionality, and operating principles are analyzed and some recommendations are made for selection purposes. A comprehensive design guideline for SIW power dividers is given in this paper through a comparative study of T- and Y-type SIW junctions. These guidelines are based on key parameters, including insertion loss, isolation, co-phase bandwidth, return loss bandwidth, and phase balancing. This study provides valuable information for selecting and designing the best possible configuration of SIW power dividers for specific applications in microwave and millimeter-wave frequency ranges. A case study of a Ku-band SIW power divider is performed for a Ku-band soil moisture radiometer SIW antenna array.

**INDEX TERMS** Insertion loss, isolation, millimeter-wave, power divider, phase balancing, RMS phase error, return-loss bandwidth, substrate integrated waveguide (SIW).

## I. INTRODUCTION

Substrate-integrated-waveguide (SIW) technique has gained huge importance in designing all microwave and mm-wave integrated circuits such as multiplexers, mixers, power combiners, and antenna feed networks [1], [2]. Compared to integrated SIW structures, conventional waveguides provide higher power capability, higher quality factor, lower loss, and wider bandwidth [3], [4], [5]. However, these waveguides' heavy and bulky structure limits their integration with other systems at microwave and mm-wave frequency domains. To merge rectangular waveguides with planar structures, some sophisticated transitions have to be incorporated, but these transitions require mechanical assembling that is very difficult and expensive at millimeter frequency.

The associate editor coordinating the review of this manuscript and approving it for publication was Wenjie Feng.

To compensate for this drawback, a planar microstrip configuration can be used, but at higher frequencies, there is radiation leakage from the microstrip lines, resulting in poor isolation and insertion losses [54]. Furthermore, microstrip lines become very thin at higher frequencies resulting in poor performance of dividers. In terms of transmission loss, waveguides are considered to be the most appropriate option compared to microstrip lines or other suspended lines.

To avoid mechanical assembling, integrated SIW technology was introduced in which metallic rows of vias/conducting holes are incorporated on the same substrate to realize bilateral edge walls [6], [7], [8]. Such transitions are done on the same substrate, so there is no need for mechanical assembly. The rows of vias act as electric shields helping to avoid any radiation leakage. This technology gives both advantages of a higher Q-factor and easy fabrication on a printed circuit board (PCB) which means that CNC machining is not required.

All other transitions, such as microstrip lines and coplanar waveguides (CPWs), can be integrated on the same substrate. Hence, a system in a package (SOP) can be integrated easily, enhancing system reliability and manufacturing repeatability.

Initially, researchers focused on embedding the SIW technique in feeding structures of many antenna types, such as parallel-plate slot array antennas. SIW feeding techniques proved to be promising candidates in terms of their practical feasibility in fabrication for millimeter-wave applications. In 1998, researchers incorporated the SIW feeding technique for the first time due to its advantages [7]. There are several feeding methods reported in the literature to excite a TEM wave in a parallel plate waveguide. These methods include horn structures, parabolic reflectors, and feed structures using non-radiative dielectric (NRD) [9], [10], [11], [12], [13], [14], [15], [16]. However, all these methods require more space to be integrated on the same radiating surface. SIW technique was initially introduced as a feeding technique and later gained significant attention as a power divider in the research field. They act as reciprocal structures and can be used as combiners as well as splitters [1], [2]. To design a functional divider, achieving low attenuation and phase balancing are the most important parameters that have to be considered.

There are different types of SIW power divider topologies which include corporate, series, multimode interference (MMI), half-mode (HM) SIW (HMSIW), QMSIW, EMSIW, radial cavity, Wilkinson, and Gysel. Each topology needs to be well investigated and understood based on a number of factors, including bandwidth enhancement techniques and reflection canceling techniques caused by abrupt SIW bend. This paper will critically evaluate each topology's advantages and disadvantages and their recent development. To date, many studies have been done on SIW power dividers that include Y or T dividers [17], [18], [19], radial cavity power dividers [20], [21], [22], [23], and multi-layer power dividers [24], [25], [26]. All these studies will be reviewed in this paper in detail.

The paper is organized as follows: Section II will demonstrate analytical equivalence between a substrate-integrated waveguide (SIW) and a rectangular waveguide, highlighting the SIW characteristics along with brief design guidelines through mathematical expressions. Section III will comprehensively overview different types of SIW power dividers based on their topologies. Section IV will present comprehensive design guidelines for designing a basic 2-way SIW power divider. This section discusses different design parameters in detail through simulations and parametric analysis. Finally, Section V concludes and recommends various options for SIW power dividers depending upon the system requirements as well as their pros and cons. This paper will develop a process for selecting SIW power dividers for specific applications e.g., power dividers with an unequal split ratio help in beamforming, while corporate power dividers are promising for easy phase equalization, and series power dividers are prioritized for frequency scanning as in leaky wave antennas.

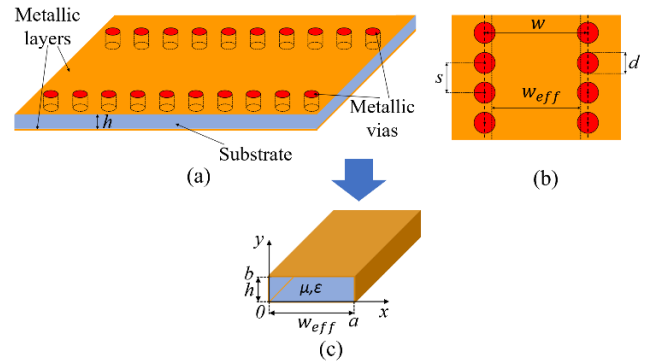


FIGURE 1. Substrate integrated waveguide: (a) isometric view, (b) horizontal cross-section, and (c) equivalent rectangular waveguide.

## II. ANALYTICAL EQUIVALENCE BETWEEN SUBSTRATE-INTEGRATED WAVEGUIDE (SIW) AND RECTANGULAR WAVEGUIDE

A substrate-integrated waveguide (SIW) comprises a thin dielectric substrate sandwiched between two solid metallic planes. Rows of metallic vias form the two conductor side-walls. The center-to-center distance of two adjacent vias is denoted by  $s$  and the via diameter is  $d$ . The width  $w$  is the center-to-center spacing between the two rows of vias. To analyze a SIW, the structure of a SIW is converted into its equivalent dielectric-filled rectangular waveguide. Then, the fundamental theory of conventional rectangular waveguides can be applied to SIWs by considering the differences between rectangular waveguides and SIWs. The configuration of a SIW and its equivalent rectangular waveguide are shown in Fig. 1. To find the equivalent rectangular waveguide for a SIW, the width  $w$  cannot be used directly as the rectangular waveguide width. The reason for that is due to the space between adjacent vias and the via shape. Thus, the effective width  $w_{eff}$  needs to be computed from  $w$ ,  $s$ , and  $d$  to build the SIW's equivalent rectangular waveguide. Given the condition of sufficiently small spacing between the vias, the effective width  $w_{eff}$  of a SIW is calculated as in [51]

$$w_{eff} = w - \frac{d^2}{0.95s} \quad (1)$$

A more refined empirical equation to compute  $w_{eff}$  that takes the ratio of  $d$  to  $w$  into account is as [52]

$$w_{eff} = w - 1.08 \frac{d^2}{s} + 0.1 \frac{d^2}{w} \quad (2)$$

As a result, the SIW in Fig. 1(a) is equivalent to the dielectric-filled rectangular waveguide with the dimensions of  $h \times w_{eff}$  as shown in Fig. 1(c). From now, one can utilize classical waveguide theory to compute the SIW's cut-off frequency for a particular model. The cut-off frequency of a classical waveguide is written as in (3), [64].

$$f_{c_{mn}} = \frac{1}{2\pi\sqrt{\epsilon\mu}} \sqrt{\left(\frac{m}{a}\right)^2 + \left(\frac{n}{b}\right)^2} \quad (3)$$

where  $m$  and  $n$  are the numbers of half-wave variations of the field in the  $x$  and  $y$  directions, respectively;  $\epsilon$  and  $\mu$  are the

dielectric permittivity and permeability, respectively;  $a \times b$  are the interior dimensions of the waveguide. In the case of a SIW here,  $a$  is  $w_{eff}$  while  $b$  is  $h$ .

However, due to the sidewall structure of SIWs, the guided wave and leakage characteristics of a SIW are slightly different from those of a rectangular waveguide counterpart. In terms of mode propagation, TM modes cannot be excited and extracted; a SIW supports only  $TE_{m0}$  modes. In  $TE_{m0}$  modes, the current on the narrow wall flows parallel with vias, therefore, the slots between vias do not cut the surface current. Hence,  $TE_{m0}$  modes can be maintained in the SIW structure. In contrast, if TM modes exist, a transverse magnetic field will generate a longitudinal surface current. The vias slots on the narrow walls will cut the current and cause radiation. Therefore, only  $TE_{m0}$  modes are preserved in the SIW structure. Consequently, the cut-off frequency for  $TE_{m0}$  of the SIW is expressed as

$$f_{c_{m0}} = \frac{1}{2\pi\sqrt{\epsilon\mu}} \frac{m}{w_{eff}} \quad (4)$$

Moreover, because of the spacing between metallic vias, the side walls cannot shield electromagnetic waves completely, as in the case of conventional waveguides, SIWs suffer from more leakage loss. Also, SIWs probably experience electromagnetic band-stop phenomena due to the periodic structure of metal posts. It is suggested that the  $s/d$  ratio should be less than 2 to reduce the leakage loss. The  $d/w$  ratio is chosen to be less than  $1/5$  to minimize the degradation of SIW dispersion characteristics [52].

### III. CLASSIFICATION OF SIW POWER DIVIDERS

SIW power dividers are widely used in microwave and mm-wave frequencies as a replacement for waveguide-like structures, resulting in compactness at such high frequencies. The main building blocks of a complete N-way power divider have three major parts: T-junctions, Y-junctions, and SIW bend. The overall performance of a power divider highly depends upon the structure of these basic building blocks. These power dividers can operate in equal or unequal split ratios depending on system requirements. Power dividers with un-equal split ratios, help in reducing the beam squinting by providing a balanced phase over the operating bandwidth.

In this study, SIW power dividers have been classified into the following categories, as shown in Fig. 2, based on their compactness, mutual coupling, additional losses due to traveling paths, and bandwidth requirements. Each category has its pros and cons and can be prioritized depending on the system design requirements.

#### A. CORPORATE (TREE) DIVIDER

This type of divider is capable of providing equal or unequal power splits depending upon the system requirements. Usually, these dividers undergo higher insertion loss because the signal has to travel longer lengths as compared to the other simpler divider topologies. Moreover, it undergoes multiple reflections at multiple bends of each stage. Y-junction

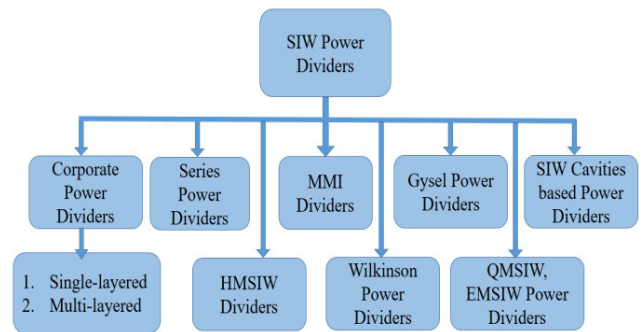


FIGURE 2. Classification of SIW power dividers.

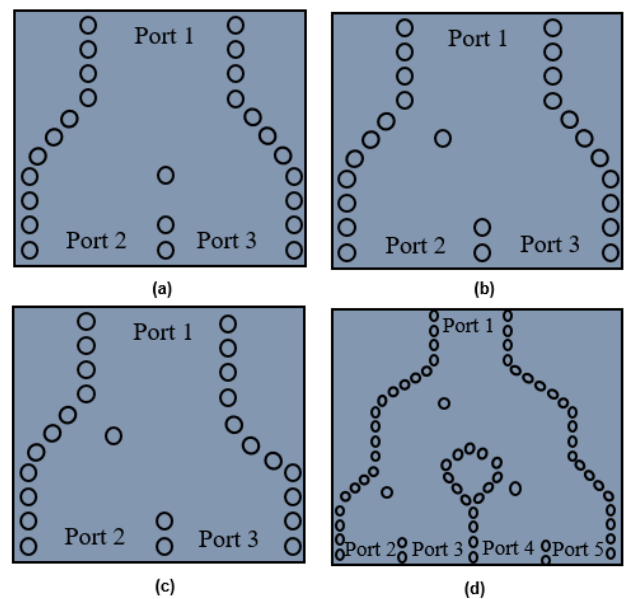


FIGURE 3. (a) Y-shaped power dividers with equal power distribution, (b) with unequal power distribution, (c) with lower SIW width to eliminate power shift (d) four-way power dividers with non-uniform power distribution [27].

power dividers are a popular type of power divider in most of the reported works. In [27], a four-way power divider with non-uniform power distribution was designed, as shown in Fig. 3. This design consists of Y-junction dividers and right-angle SIW bends. The non-uniform power division is achieved by displacing the center inductive pole to a different position. Non-uniform power distribution plays a vital role in suppressing side lobe levels and shaping beams in a particular direction. Fig. 3 (a) shows a uniform Y-junction power divider with an inductive pole placed in the center. Fig. 3 (b) shows a non-uniform Y-divider with an inductive pole displaced towards the left side. Fig. 3 (c) shows the same Y-divider but with lower SIW width. This design's dimensions are not symmetric, which is obvious from the right-sided SIW bend. Lower SIW width helps eliminate the phase shift. On the other hand, it will disturb the power distribution level too. So, both factors i.e., SIW width and via position, have to be optimized to get desired results. Fig. 3 (d) shows the design of a four-way power divider with non-uniform power distribution. Although the Y-type

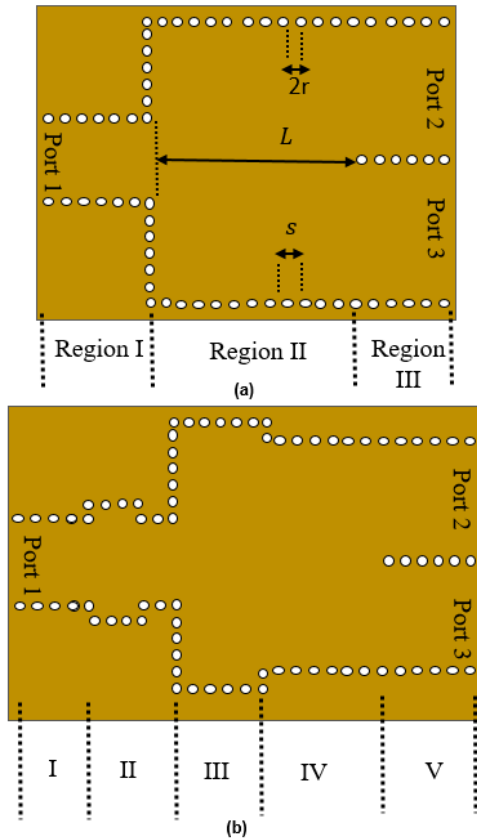


FIGURE 4. (a) Basic Y-shaped divider, (b) Y-shaped power divider to avoid sharp stop peak with equal power distribution [30].

divider helps in enhancing bandwidth, at the same time, it has a drawback of sharp stop peaks in the operating bandwidth [28], [29], [63]. To avoid this limitation, the researchers tried to introduce  $TE_{10}$  and  $TE_{30}$  modes in the coupling region [30]. They have divided the complete Y-divider into three regions i.e., Region I consists of input ports, and Region II is a coupling region between the input and output ports. Region III consists of output ports. In the coupling region, E-field distribution has been changed by doing amendments in SIW walls. The new proposed design consists of 5 regions instead of 3, as shown in Fig. 4.

T-type two-way power divider and Y-type two-way power divider models have been designed and optimized in [18]. The one-step normalized design curves for both topologies have been proposed in this paper. These curves can help in optimization techniques for designing multi-way power dividers. A bandwidth of 25.2% was achieved by the Y-junction and a bandwidth of 10.2% was achieved by the T-junction.

Corporate dividers can be single-layered as well as multi-layered. Multi-layered topology provides the benefit of higher compactness as compared to single-layered configuration.

### 1) SINGLE-LAYERED POWER DIVIDERS

There have been a huge number of publications on single-layered corporate power dividers [19], [31], [32],

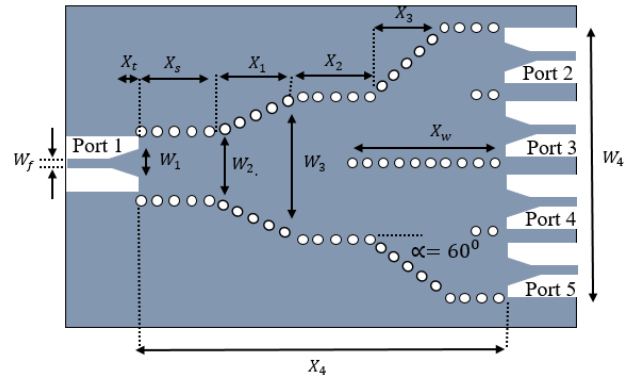


FIGURE 5. Structure of the proposed four-way SIW power divider [31].

[33]. Researchers have incorporated different techniques to achieve better impedance matching throughout the operational bandwidth. These methods include the introduction of inductive posts, right-angle SIW bends, and curved SIW bends instead of abrupt corner bends. One of the researchers, Karimabadi [31], proposed a 4-way corporate power divider by using only Y-junction dividers and right-angle SIW bends, as shown in Fig. 5. This design achieved a bandwidth of 40% from 4.5 GHz to 6.8 GHz. In this power divider, the overall substrate integrated waveguide is divided into two parts by the main conducting wall, as shown in Fig. 5. Each part is further divided into two parts to make a complete 4-way power divider. Microstrip-to-waveguide transitions have been incorporated at each input and output port to yield a planar feed structure [31]. Along with the achieved wider bandwidth, there were some phase and amplitude mismatches at different ports over the operating bandwidth.

Similarly, another SIW slot array antenna in the Ku band was developed with a  $1 \times 8$  SIW power divider along with an  $8 \times 10$  slot array antenna [32]. This power divider has been designed by using Y-type power dividers, and right-angle SIW bends instead of inductive posts, as shown in Fig. 6. Major operating parameters of power dividers, such as operating bandwidth and return loss, are highly dependent upon one design parameter. The design parameter is the distance of the input port from the conducting wall that divides each path into two. This length is denoted by L. For this design, there is a deviation of operating frequency of around 4 MHz between simulated and measured results.

Another design of a single-layer 16-way power divider was designed by using 8 two-way Y-dividers, 7 two-way T-dividers, and 14 SIW bends [19]. In this design, the author incorporated novelty in Y-type dividers by keeping the widths of all ports equal. This is done to avoid a sharp stop peak in the operating band.

Furthermore, the placement and diameter of inductive posts were optimized to get better return loss and minimum reflections. This research paper used guidelines from an already published paper [18]. Zhang Cheng used this power divider with uniform distribution for a linearly tapered slot antenna (L TSA) [33].



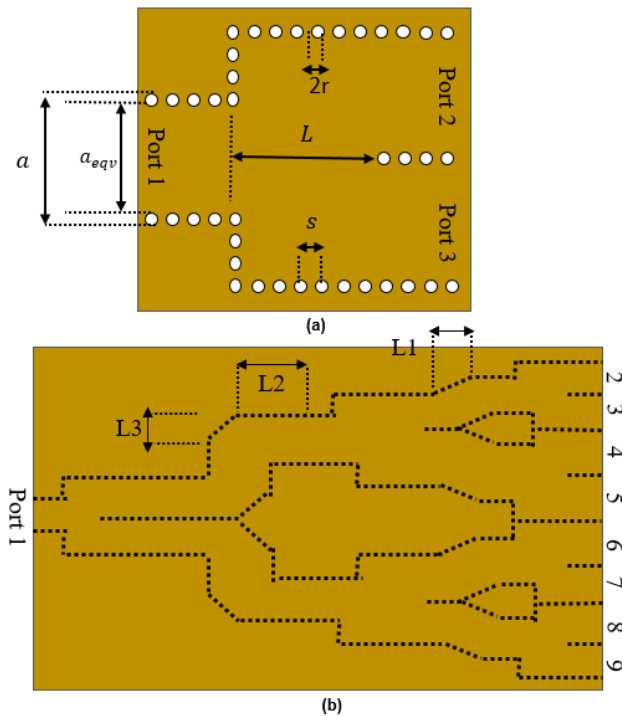


**FIGURE 6.** (a) Feeding network geometric parameters, (b) an 8-way uniform power divider [32].

## 2) MULTI-LAYERED POWER DIVIDERS

Multi-layer configurations have a promising performance in reducing overall divider size to gain compactness at higher frequencies, compared to single-layer configurations.

One approach to designing a multi-layer structure is to utilize a single-layer design and translate it into a multi-layer structure. This approach can reduce the overall size to half. For instance, the size of the Antenna array designed in [32] has been reduced to half by changing the single-layer configuration to a multi-layer configuration, engraving a coupling slot between the layers [34]. The position and size of the coupling slot were optimized following the guidelines from [35] to obtain a better coupling level with an insertion loss of approximately 1 dB. Also, in this paper, via transition and aperture transitions of SIW structure have been modeled as lumped components (inductors and capacitors). By evaluating the values of lumped components, the test fixtures were characterized by S-parameters vs. frequency providing a validity range.

In some designs, SIW cavity has also been introduced among multi-layers to suppress the surface waves. This SIW cavity also acts as a radiator that increases the radiation resulting in enhanced radiation efficiency and gain [36], [37].

A single-layer SIW feed network incorporated with only wideband T-junctions for a  $4 \times 4$  multi-layered cavity-backed aperture-coupled patch antenna array was presented in [38] for V-band applications. Despite the radiating-slots performance, the feed network was found to be complex due to the multiple rows of vias required in a single wall to minimize radiation leakage. In response to the design complexity, a

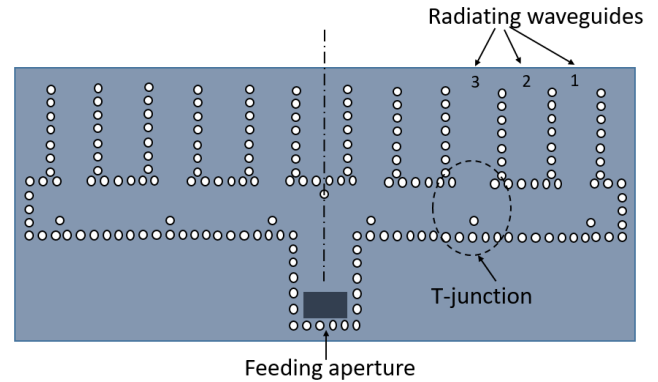


**FIGURE 7.** Feed structure of a slotted post-wall waveguide array [50].

multi-layered compact SIW that incorporated the feed network for 256 antenna array elements was proposed in [39]. This new design consists of two layers. One layer includes the power divider for 64 elements as in the previous design but without multiple rows of vias. The second layer included 64 sets of a  $2 \times 2$  subarray split for 256 radiating elements, including one coupling slot in each  $2 \times 2$  subarray to couple the power from layer 1 to layer 2.

## B. SERIES DIVIDERS

Series dividers gained huge attention in recent past years. In this topology, the signal needs to travel shorter lengths as compared to corporate dividers, resulting in lower insertion loss and lower radiation leakage. There are a few series power dividers reported in the literature [50], [58], [59], [60], [61], [62] to utilize some benefits of compactness and less complexity despite some drawbacks that are linked to it. The first drawback is its higher external mutual coupling due to the power divider's lower co-phase bandwidth, which also resulted in broadened beam width at the E-plane. In addition, external mutual coupling was found to be high, which resulted in convergence during array synthesis. Despite its compactness, a series feed network exhibits lower co-phase bandwidth, making it frequency sensitive. As the frequency varies, the antenna beam tends to tilt. Such an attribute can be utilized in frequency-scanning arrays but is usually undesirable.

A 6-way series power divider was reported in [50] by Xu. T-junctions were incorporated into the design as building blocks of the multi-way divider as shown in Fig. 7. All junctions were separated by guided wavelength to match the phases of all the ports along the y-axis. To avoid reflection caused by coupling windows, one post is introduced in front of each window.

## C. HMSIW DIVIDERS

A basic SIW configuration has a high width-to-height ratio that leads to more space occupation when integrated with other miniaturized structures. To reduce the size of SIW by almost half, an improved guided wave structure called half mode substrate integrated waveguide (HMSIW) came into existence. This technique was based on the fact that the max-

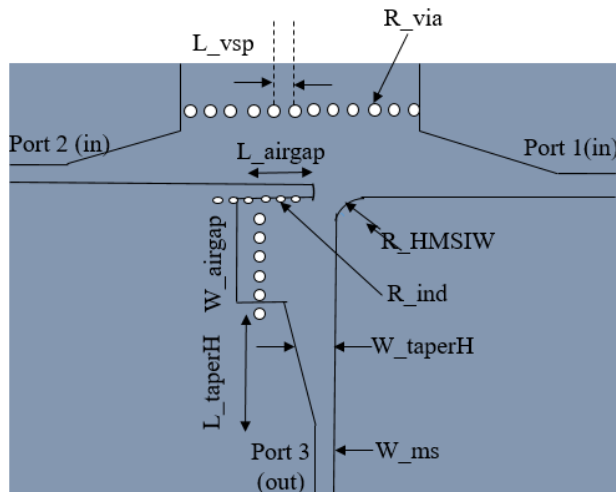


FIGURE 8. The layout of the proposed T-junction [42].

imum electric field of SIW is found vertically to the direction of propagation. The center plane of SIW can be considered to act as a magnetic wall. So, the overall SIW structure can be cut in half along the direction of propagation, keeping the mode  $TE_{10}$  intact [40]. In 2006, the concept of HMSIW was proposed by Hong et al. [41]. After that, this term gained huge attention in the research area. For the very first time, a T-junction HMSIW design was published [42]. In this research paper, the author used a basic T-junction HMSIW block to realize a multiport divider. Furthermore, an air gap was used in the top metal plate for an equal power split ratio, as shown in Fig. 8.

Additionally, to avoid any additional energy coupling, a row of vias was introduced along the air gap. This design proved to be flexible enough to yield an unequal split power ratio by changing the air gap dimensions. This work presented in [42] summarizes three structures, i.e., H plane T-junction, linear hybrid four-way power divider, and series four-way power divider.

Similarly, by using HMSIW, combiners at higher frequencies were proposed in [40]. They have used identical HMSIW-to-microstrip transitions to realize a four-way spatial power combiner at Ka-band. A multi-layer four-way out-of-phase power divider was proposed in [43]. In this research, the author introduced a novel approach by dividing each input SIW vertically and each SIW is then laterally coupled to output HMSIW. Using this technique,  $-7.0 \text{ dB} \pm 0.5 \text{ dB}$  insertion loss and return loss of about  $-10\text{dB}$  in a frequency band of 7.63 GHz to 11.12 GHz were achieved. Another technique known as image transition was used in [44] by using the HMSIW technique, as shown in Fig. 10.

Again, air slots and rows of vias are etched in this structure to meet the purpose.

#### D. MMI DIVIDERS

The effect of spatial self-imaging was discovered in 1836 by Talbot [45]. This phenomenon is generated by periodic

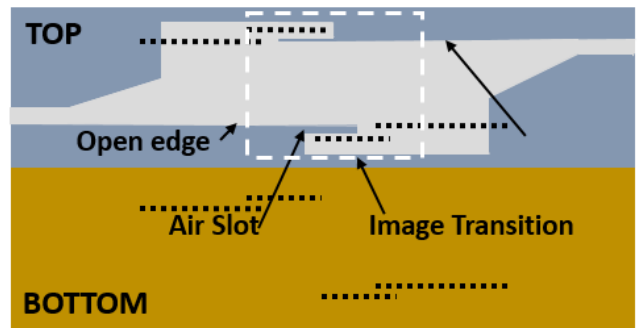


FIGURE 9. Proposed ITHMSIW topology [44].

objects which are illuminated by coherent light. It was discovered later that instead of spatial interference by Talbot effects, interference of multiple modes in optics could also be created by graded-index waveguides. In a multimode waveguide, input signals can be reproduced in different images in the direction of propagation. At first, the overall power is divided into different modes with different phase velocities. Each field associated with each mode travels along the direction of propagation. All modes accumulate and meet certain phase requirements at a particular transverse plane, creating a final image at output. To form multiple images of 2D objects, many integrated optical applications have used this technique of self-imaging [46], [47], [48], [49]. Researchers have used this technique in designing power splitters, combiners, and modulators.

A  $1 \times 6$  power divider at 25 GHz was presented in [49]. From each input waveguide to the output, they achieved an insertion loss of around  $-9\text{dB}$  and an isolation of better than  $-10\text{dB}$  between ports but with limited operating bandwidth. Although MMI technology offers lower insertion loss, there are some challenges associated with it i.e., less compactness and limited bandwidth. These challenges are needed to be investigated further to make MMI dividers feasible enough to be used at microwave and mm-wave frequency bands.

#### E. WILKINSON DIVIDERS

As a nature of a 3-port network, a 3-port power divider cannot meet the requirements of lossless and being matched at all the ports concurrently. A Wilkinson power divider is a lossy network that provides good matching at all the ports and a high degree of isolation between output ports [53].

Wilkinson Power divider provides low insertion loss, wide bandwidth, and very good VSWR. One drawback associated with Wilkinson dividers is their lower power handling capability. This is due to the presence of isolation resistance. This limitation has been catered to by introducing Gysel power dividers, discussed in the following section.

Conventionally, Wilkinson power dividers have been realized in microstrip technology. The first design reported in [54] is an HMSIW H-plane Wilkinson power divider. The circuit utilized one SIW as an access section and two HWSIW as quarter-wave impedance transformers. The  $100 \Omega$  resistance was connected to the ends of the two

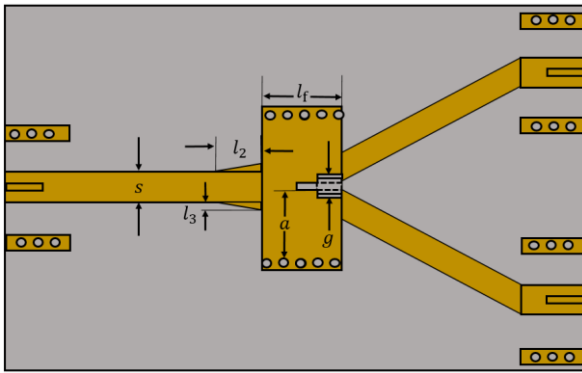


FIGURE 10. SIW Wilkinson power divider [54].

HWSIW, as shown in Fig. 10. The return losses and isolation better than 10 dB were claimed over 40% bandwidth centered at 10.5 GHz.

Another design of the Wilkinson power divider was reported in [55]. It was considered a true SIW Wilkinson configuration. It strictly followed the Wilkinson power divider principle. The design used a non-radiating slot in the center to separate the two HMSIW quarter-wave impedance transformers. The measured results recorded at 15 GHz were the output return losses of 14.5 dB, the isolation between output ports of 17 dB, and the insertion loss of about 4 dB. In [56], two ring-shaped SIW Wilkinson power dividers were proposed by adding transmission lines to connect isolation resistors. The designs solved the problems of varying impedance without changing cut-off frequency by adding one more layer under the circle or using the HMSIW structure. Also, the problem of integration of isolation resistance was studied and addressed. The design prototype achieved a 25% bandwidth at the 10 dB reference with a loss of less than 0.75 dB. The recent work reported in [57] proposed a new modified architecture of the Wilkinson power divider. The design utilized the same width lines for the access, the quarter-wave impedance transformer, and the arms for connecting isolation resistance. The lines have the same impedance and cut-off frequencies; thus, they can avoid the presence of high-order modes. Also, the number of isolation resistors was investigated for better isolation. The design gained a 20-dB isolation bandwidth of 18% centered at 10 GHz with less than 0.3 dB losses.

## F. GYSEL POWER DIVIDERS

Wilkinson and Gysel power dividers have gained more attention among existing power dividers. Although the classic Wilkinson power divider offers low insertion loss, wide bandwidth, and good VSWR, its high-power handling capacity is limited. It is due to the distributed capacitance between an isolated resistor and the ground. On the other hand, the Gysel power divider has been widely researched in recent years due to its high-power handling capability, compact size, and low loss [63], [64], [65], [66], [67], [68], [69], [70], [71], [72], [73], [74], [75], [76]. A standard Gysel power divider (GPD) consists of quarter-wave transmission lines with three

different impedance values in order to achieve the required power division and isolation. The short-ended resistors in GPD can be easily replaced by external high-power loads.

Furthermore, instead of single-band power dividers, the demand for multiband power dividers has become inevitable due to the rapid development of microwave communication systems. Some research has been done in order to realize dual-band Gysel power dividers. For instance, utilizing composite right/left-handed (CRLH) transmission lines (TLs) [66], incorporating coupled lines [70], using open/short-ended stubs [71], [72], [73], using fixed characteristic impedance [74], and with different electrical lengths [75].

At the microwave frequency range, incorporating microstrip lines (MSL's) with different widths can cause higher order modes and unwanted radiations at the level of discontinuities of MSL's. In [74], the authors have used transmission lines with fixed characteristic impedances to avoid fabrication limitations and parasitic capacitances. Keeping microstrip line widths fixed, the lengths of MSL's have been changed in order to realize a simple and compact Gysel power divider. The above mentioned papers have realized dual-band Gysel power dividers but with equal power division ratios at all arms. In [75], an unequal power division ratio has been achieved by selecting proper electrical lengths and line impedance of transmission lines.

Apart from the high-power handling capacity (PHC) of Gysel power dividers (GPD), they offer very limited bandwidth. In order to eliminate this drawback, the author has proposed the idea of using a multi-sectional design [76] instead of a single-section design, as shown in Fig. 11. Additionally, the large number of sections inherently comes with a large number of resistors which will facilitate the overall higher power handling capacity.

## G. QMSIW POWER DIVIDERS

Quarter-mode substrate integrated (QMSIW) power dividers are realized by bisecting the conventional SIW twice along the symmetrical magnetic wall. The original characteristics of SIW remain intact even after bisection. The overall size of SIW is reduced by almost 75% through this kind of bisection. At microwave frequencies, QMSIW power dividers offer more compactness as compared to conventional SIW or HMSIW designs. In [77], QMSIW power dividers have been proposed with in-phase and out-of-phase topologies. In order to achieve in-phase performance, two inductive windows are introduced in the single-layered substrate. While, for out-of-phase performance, a multi-layer SIW structure has been proposed that helps reverse the phase to 180 degrees between the two outputs. Furthermore, QMSIW technology provides excellent filtering capability keeping the overall size compact. In [78], a triple-mode filter has been investigated based on QMSIW technology. In order to get desired bandwidth and resonant modes, a small via-hole is introduced at the lower right corner of the triangular section of QMSIW as shown

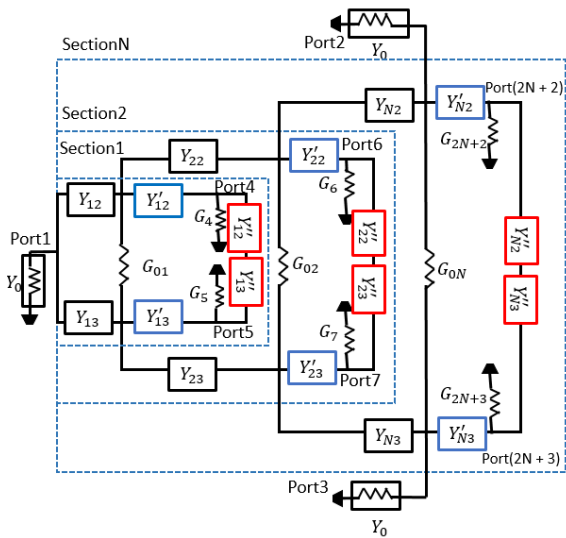


**FIGURE 11.** Block diagram of a multi-sectional Gysel Power divider (GPD) [76].

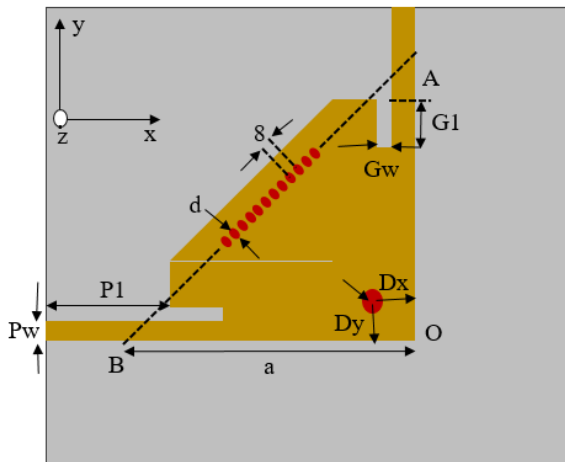


**FIGURE 12.** Geometrical diagram of a triple-mode filter incorporating QMSIW [78].

in Fig. 12. The placement of the hole plays a very important role in achieving desired TM modes. Another technique of ridged [79] and folded ridged QMSIW [80] has been investigated in past research work. These techniques further reduce the overall size of QMSIW. In [81], a ridged QMSIW cavity is folded to reduce the covered area by 92%. In this paper, a dual-band band-stop filter is designed by adding two tunable capacitances with two different resonators. These resonators are combined through an impedance inverter to realize a dual-band filter.

**H. EMSIW POWER DIVIDERS**

Eight-mode substrate-integrated (EMSIW) power dividers are realized by bisecting the conventional QMSIW twice along the fictitious symmetrical magnetic wall [82]. The overall size reduces drastically, but the resonant frequencies remain intact. EMSIW offers an 87.5% size reduction as compared to the conventional SIW. In [83], a wide-band

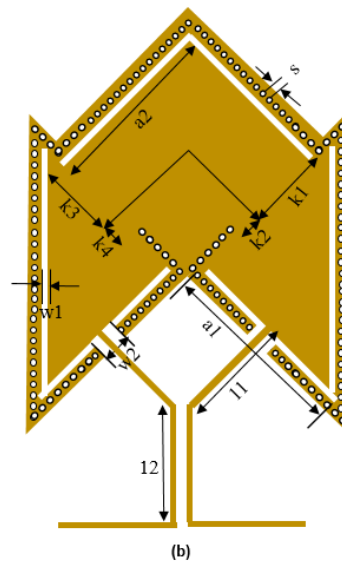
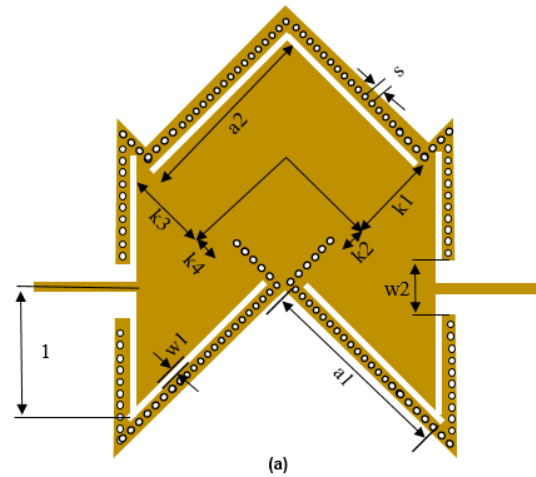


**FIGURE 13.** (a) Geometrical diagram of a third-order band pass filter using EMSIW. (b) Modified structure by increasing coupling between source and load [84].

LTCC bandpass filter has been proposed using the EMSIW technique. Low-temperature ceramic con-fire (LTCC) plays a major role in package size reduction. That’s why this paper has introduced a very compact design using both techniques of LTCC and EMSIW. Furthermore, in [84], a third-order band-pass filter is designed using QMSIW and EMSIW together, as shown in Fig. 13. In the modified structure, the coupling between the source and load has been increased in order to achieve better frequency selectivity.

**I. SIW CAVITIES POWER DIVIDERS**

Substrate integrated waveguide cavities are used for better isolation as well as better filtering functionality. For millimeter wave (mm-wave) bands, filters are of huge importance to suppress the out-of-band noise and improve overall wireless communications. In [85], a triangular SIW cavity is used in order to design a SIW filtering power divider as shown in Fig. 14. Conventional SIW power divider ignores



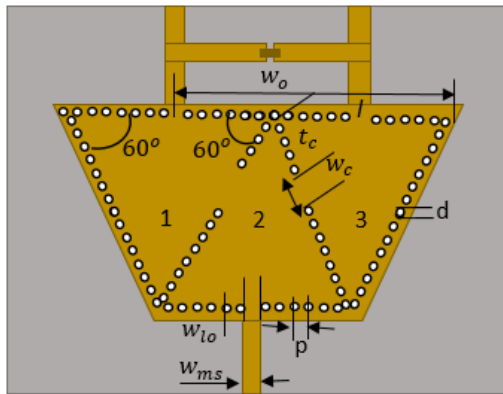


**FIGURE 14.** Geometric diagram of a SIW filtering power divider using triangular SIW cavity [85].

the coupling effect between the ports. This paper incorporates an isolation resistance of 100 ohms in order to achieve higher isolation between the output ports. Similarly, in [86], two TE<sub>101</sub> mode SIW cavities have been used in order to design a two-way multi-layer filtering power divider. Another advantage of this design is better isolation which has been achieved by adding an isolation resistance between the output ports. A rectangular coupled slot is used for better impedance matching between the micro-strip line and SIW.

In [87], a pre-defined filtering power divider has been used to investigate a SIW filtenna array. Filtenna is basically a combination of an antenna array with a filter. It plays a vital role in improving the performance of mm-wave systems. Intensive research has been done on filtenna arrays based on SIW cavities [88], [89], [90], [91], [92], [93]. The proposed designs in these papers are not cost-effective and simple due to their multi-layer configurations. Furthermore, the feeding networks in these research papers use uniform power distribution that causes high side lobe levels. This paper [87], introduces non-uniform power distribution in order to suppress high side lobe levels. The filtering power divider (FPD) consists of two SIW cavities, including TE<sub>101</sub> and TE<sub>301</sub> modes. These cavities are interlinked with each other in such a way that TE<sub>301</sub> distributes the overall energy into three output ports. These ports are then connected to cavity 2 for further power distribution by the ratio of 1:3:1.

**J. OVERALL PERFORMANCE COMPARISON**

All possible substrate integrated waveguide power dividers have been discussed along with their performance parameters in this section. In order to get an overall performance comparison among all types of SIW power dividers, the key parameters are listed below in Table. I.

**IV. DESIGN GUIDELINES**

This section provides comprehensive design guidelines through a critical analysis of the basic building blocks of SIW power dividers. In order to give deep insight to readers, parametric analysis is presented for 2-way Y-type and T-type SIW power dividers. Some important design curves, showing

**TABLE 1.** Key parameters of different SIW power dividers.

Category	Fractional Bandwidth	Insertion Loss	Compactness
Corporate [30] [31]	Widest of all (51 %) (40 %)	Higher (-6 dB) (-7 dB)	Lowest of all Less compact Less compact
Series [59]	Narrow (> 6 %)	Lower (< -4.5 dB)	Less compact -
MMI [49]	Narrow (~ 7.5 %)	Lower (-9 dB)	Less compact -
HMSIW [43]	Narrow (~ 18 %)	Lower Lower than MMI, Series	50 % more than SIW -
Wilkinson [53]	Wider than Series, MMI (64 %)	Lower (~ -4 dB)	More compact than SIW More compact
Gysel [63]	Narrow (~ 35 %)	Lower (-3 dB)	Comparable to Wilkinson -
QMSIW [78]	Narrower than SIW (38 %)	Lower than SIW (-2 dB)	75 % more compact than regular SIW More compact
EMSIW [82]	Narrower than SIW (24.2 %)	Lower than SIW (-2.8 dB)	90 % more compact More compact than all
SIW cavity-based [85]	Narrowest of all (6.59 %)	Lower than SIW (-3.5 dB)	Less compact than QMSIW, EMSIW -

return loss and insertion loss, are plotted through this investigation. For instance, the reflections caused by SIW bends can be mitigated using three different methods: i) introduction of induction poles at the SIW bends, ii) using right-angle SIW bends, and iii) using swept-arc SIW bends with optimized angle. This section analyzes and compares all these methods in terms of the reflection coefficient. Finally, a parametric analysis of some important variables is also presented, giving clear directions for designing SIW power dividers. These parameters include SIW width, via diameter, and induction pole placement.

**A. Y-TYPE 2-WAY SIW POWER DIVIDERS**

This basic 2-way power divider, shown in Fig. 15, has been investigated completely by parametric analysis of some important design parameters in the CST Microwave studio platform. These parameters include SIW width, SIW bends, and reflection-canceling poles. All the results have been critically analyzed to get a better comparison. This detailed comparison will help readers to have a deep insight into designing any kind of SIW power dividers.

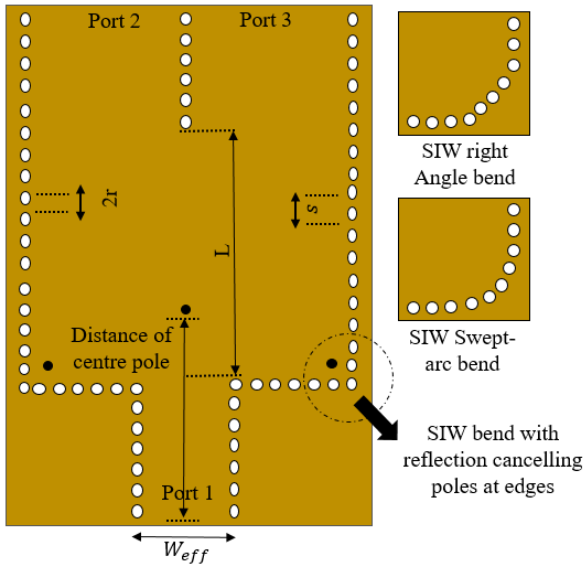
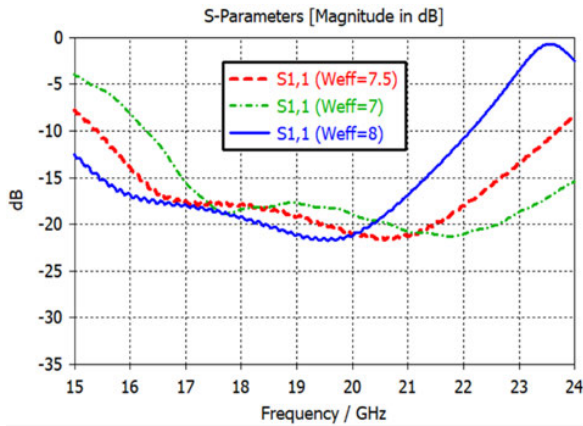
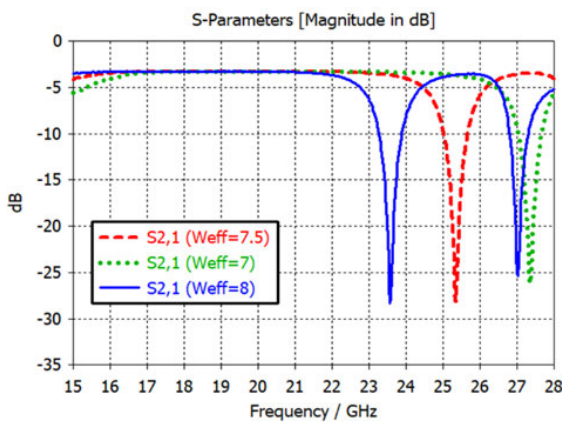


FIGURE 15. Geometry of basic SIW 2-way Y-type power divider with design parameters.



(a)

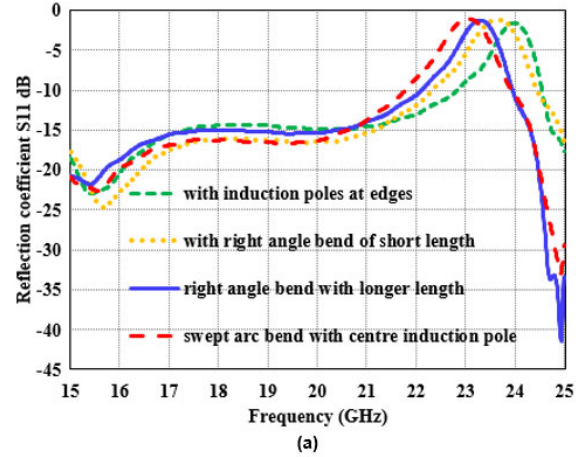


(b)

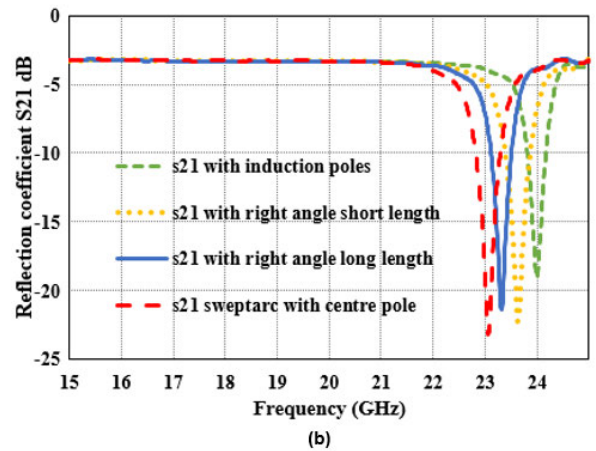
FIGURE 16. S-parameters for different values of effective SIW widths (a). Return loss  $S_{11}$  (b).  $S_{21}$  transferred power.

1) EFFECT OF EFFECTIVE SIW WIDTH

The effective width of SIW power dividers is the most important parameter to maintain the operating bandwidth at the corresponding frequency range. Furthermore, the choice of



(a)



(b)

FIGURE 17. S-parameters for different SIW bends (a). Return loss  $S_{11}$  (b).  $S_{21}$  transferred power.

via diameter ( $d$ ) along with via spacing ( $s$ ) has a greater impact on the overall performance. The empirical formulas given in (1) and (2) are extracted keeping in view the importance of the  $s/d$  and  $d/W$  ratio. As the sidewalls of SIW, are made of periodic arrays of metallic posts, some unwanted leakage loss occurs due to via spacing. If the distance between consecutive posts and their diameter are carefully selected, the extra energy leakage becomes nearly negligible. In order to avoid extra leakage loss, the  $s/d$  ratio must be kept less than 2 and the  $d/W$  ratio must be less than  $1/5$ . Additionally, the distance of the input port from the output ports ( $L$ ), has a greater impact on achieving the lowest level of return loss.

As a first step in designing any SIW power divider,  $w_{eff}$  must be calculated through (2). As illustrated in Fig. 16, overall operating bandwidth shifts towards a lower frequency range with an increase in  $w_{eff}$  of SIW. This graphical representation reveals the fact that effective SIW width ( $w_{eff}$ ) is inversely proportional to the operating frequency, as mentioned in (4).

2) EFFECT OF SIW BENDS

Once effective SIW width is calculated and optimized via distance and via diameters, the next step is the selection of SIW bends. There are 3 different methods of incorporating

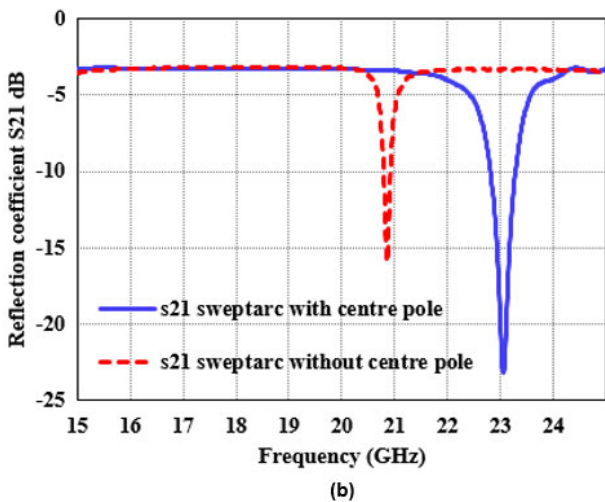
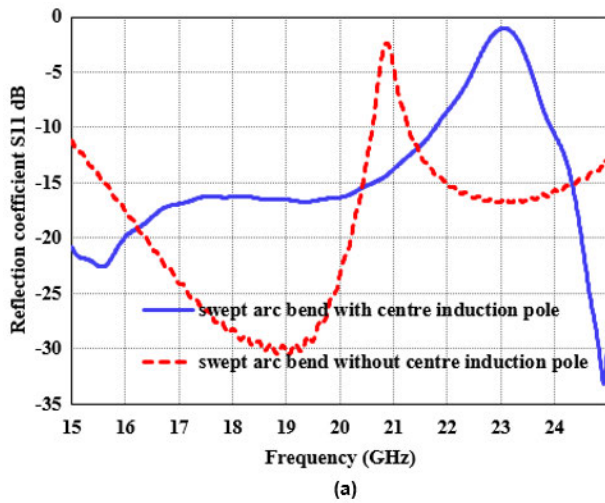


FIGURE 18. S-for center inductive pole (a).  $S_{21}$  transferred power (b). Return loss  $S_{11}$ .

SIW bends i.e., Sharp SIW bends with reflection-canceling poles, right-angle bends with optimized length, and swept-arc bends. Every type provides its benefits along with some limitations. As shown in the graph below in Fig. 17, swept-arc and right-angle SIW bends provide better return loss but limit the operational bandwidth to the lower operating frequencies. If a system has to be designed in the Ku-band, swept-arc bends are more promising than all other types. Similarly, right-angle bends prove themselves to be suitable for achieving better return loss but with optimized bending length.

### 3) EFFECT OF INDUCTION POLE AT CENTER

Reflection-canceling inductive poles at the edges and center play a vital role in the overall performance of SIW power dividers. The center inductive pole defines the higher cut-off frequency and returns the loss level. If a system needs to be designed with wider bandwidth and a return loss level of around  $-15\text{dB}$ , a center inductive pole with an optimized radius and distance from an input port helps achieve the goal. On the contrary, if the desired operating bandwidth of a system

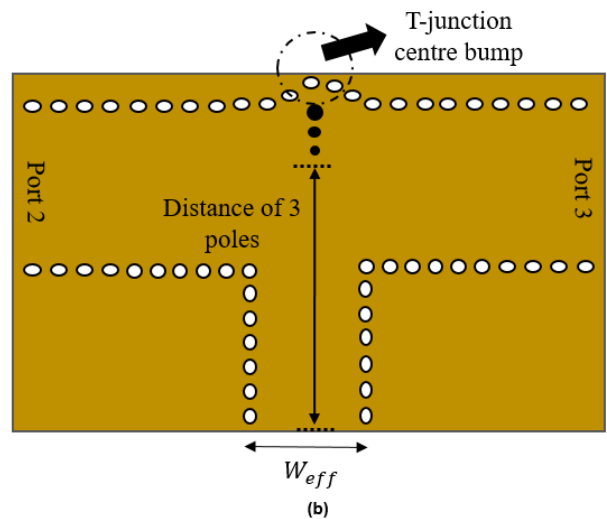
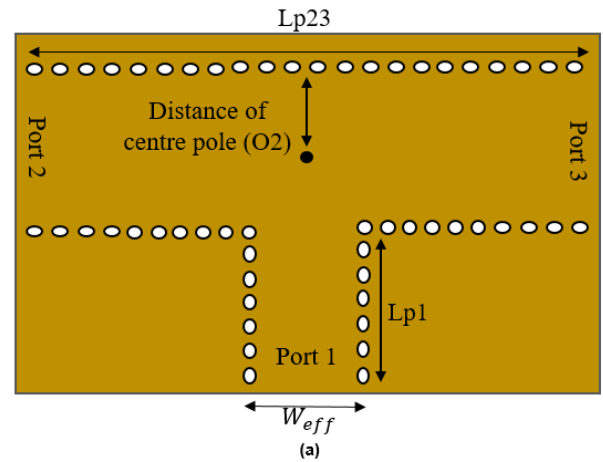


FIGURE 19. (a) The geometry of basic SIW 2-way T-type power divider with design parameters. (b) Introduction of center triangle.

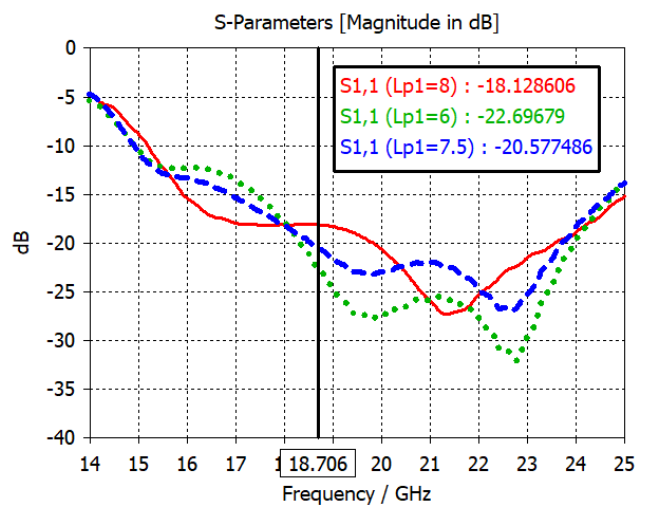
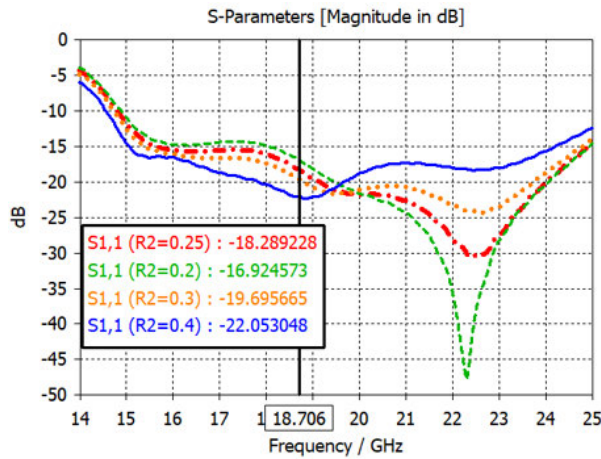


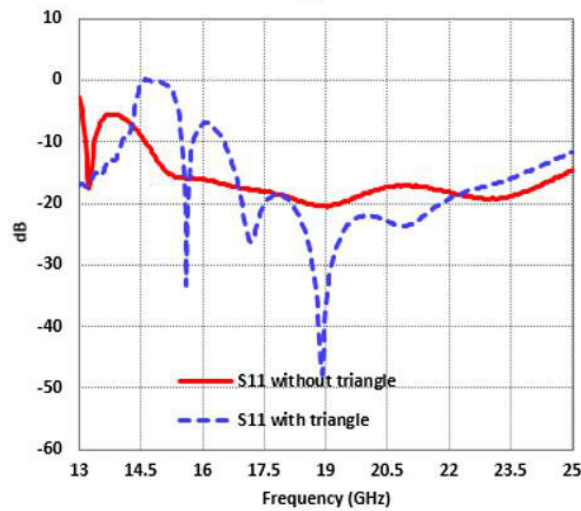
FIGURE 20. S-parameters for different input port lengths.

is limited, e.g., Ku-band (18.7 GHz), the SIW power divider without an inductive pole at the center offers a return loss better than  $-30\text{dB}$  at the required bandwidth, as shown in graphs given in Fig. 18. The dotted line curve in Fig. 18 (a)





(a)



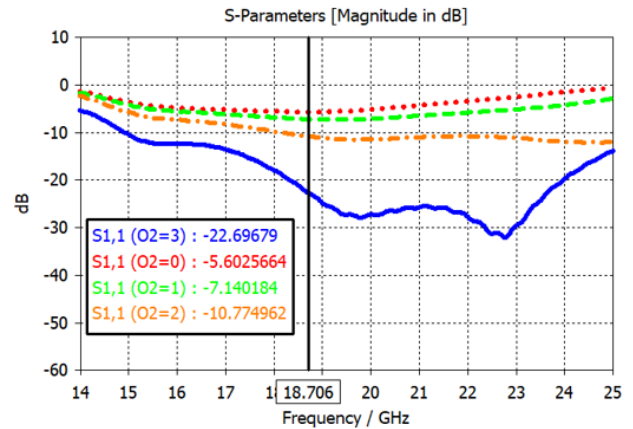
(b)

FIGURE 21. (a)  $S_{11}$  for different radii of the center pole, (b) For introducing the center triangle.

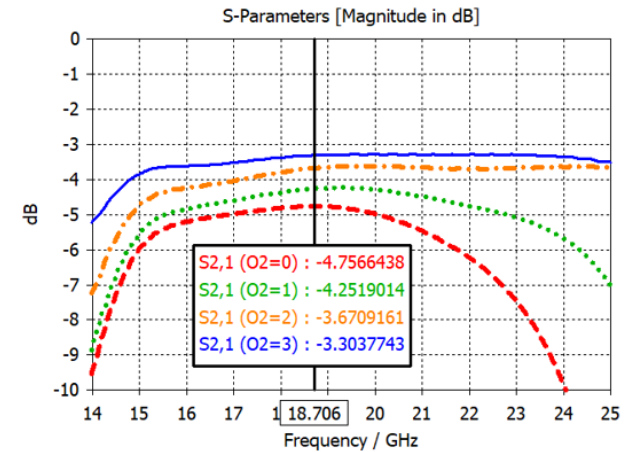
(corresponding to the design without center inductive pole) shows a return loss close to  $-30$ dB but with a narrower bandwidth. That means if the system does not require a wide bandwidth, the center inductive pole should be avoided to achieve better return loss.

**B. T-TYPE 2-WAY SIW POWER DIVIDERS**

Similar to the Y-type SIW power divider, the T-type SIW power divider shown in Fig. 19, has also been investigated well to get a deep insight into design parameters. This type of divider has been analyzed depending upon different design parameters i.e. input and output port lengths ( $L_{p1}$ ,  $L_{p2}$ ), different radii of the center inductive pole ( $R_2$ ), and distance of inductive pole from the upper SIW wall ( $O_2$ ). These parameters play a vital role in achieving desired levels of return loss, and insertion loss within the operating bandwidth. The optimized value of Input port length achieves better return loss with very less change in overall operating bandwidth. Similarly, the center pole radius choice specifies the operating range of frequencies with minimum return loss achieved. The



(a)



(b)

FIGURE 22. S-parameters for different distances of the center inductive pole (a).  $S_{11}$  (b).  $S_{21}$ .

effect of all these parameters has been elaborated well with the help of graphs.

1) EFFECT OF INPUT PORT LENGTH

This parametric analysis will give a deep understanding of the effect of the length of the input port on return loss and operating bandwidth. As shown in Fig. 20, decreasing the length of the input port results in achieving better return loss, especially at Ku-band and other adjacent frequencies. It is obvious from the graph that there is no significant change in operating bandwidth.

2) EFFECT OF DIFFERENT RADII OF THE CENTER INDUCTIVE POLE ( $R_2$ )

The center inductive pole is of much importance to achieving the optimized performance of the SIW power divider. There are 2 different methods of achieving better return loss. One is to introduce a single inductive pole at the center, and the second method is to introduce a triangle in between the output ports along with the center inductive pole. These two methods are compared well through a graphical representation of return loss, depicted in Fig. 21. It can be seen that by introducing a triangle in the center of two output ports, return



loss of 20 dB and 35.5 dB were achieved at the desired band (16.5–22 GHz) and 18.7GHz (ku-band), respectively.

### 3) EFFECT OF THE DISTANCE OF THE CENTER INDUCTIVE POLE FROM THE UPPER SIW WALL (O2)

Placement of the center inductive pole plays a vital role in achieving optimized results for return loss as well as transferred power between output ports. It is evident from the graphs given in Fig. 22 that the optimized distance of the center pole from the upper SIW wall gives optimum results for  $S_{11}$  and  $S_{21}$ . All other parameters majorly affect return loss, but this factor strongly influences both  $S_{11}$  and  $S_{21}$ .

## V. CONCLUSION

This paper gives an overview of different types of SIW power dividers. The overall performance of each topology greatly depends upon the selection of SIW bends, induction poles, and their placements. These factors must be considered to get the desired bandwidth, return loss, and balanced phase. The different SIW power dividers can be summarized with their advantages and disadvantages as follows:

1. In designing feed networks for different antenna arrays, corporate SIW power dividers are the best choice for suppressing side lobe levels (SLLs) over the operating bandwidth without any beam squinting.
2. Suppressing side lobe levels can be possible by achieving an unequal split ratio through corporate dividers but at the cost of lower compactness and poor isolation.
3. These limitations caused by corporate dividers can be overcome by using a multi-layered configuration.
4. To achieve lower insertion loss, series power dividers are more promising compared to the corporate SIW power dividers.

To date, corporate power dividers have received great research interest, but other topologies need intense investigation to design the optimal system. This can lead to having more options for selecting a suitable type of power divider for specific applications.

This study has provided a comprehensive review of all types of SIW power dividers, along with their important design guidelines. This paper will help readers to have a clear vision of SIW technology.

## ACKNOWLEDGMENT

The authors would like to thank Jane Moodie for her assistance in proofreading the article.

## REFERENCES

- [1] D. Deslandes and K. Wu, "Integrated microstrip and rectangular waveguide in planar form," *IEEE Microw. Wireless Compon. Lett.*, vol. 11, no. 2, pp. 68–70, Feb. 2001.
- [2] K. Wu, "Integration and interconnect techniques of planar and non-planar structures for microwave and millimeter-wave circuits—Current status and future trend," in *Proc. Asia-Pacific Microw. Conf.*, 2001, pp. 411–416.
- [3] E. Mehrshahi, M. Salehi, and R. Rezaiesarlak, "Substrate integrated waveguide filters with stopband performance improvement," in *Proc. Int. Conf. Microw. Millim. Wave Technol.*, May 2010, pp. 2018–2020.
- [4] G. Angiulli, E. Arnieri, D. D. Carlo, and G. Amendola, "Fast nonlinear eigenvalues analysis of arbitrarily shaped substrate integrated waveguide (SIW) resonators," *IEEE Trans. Magn.*, vol. 45, no. 3, pp. 1412–1415, Mar. 2009.
- [5] L. Bing, W. Hong, Z. Kuai, X. Yin, G. Luo, J. Chen, H. Tang, and K. Wu, "Substrate integrated waveguide (SIW) monopulse slot antenna array," *IEEE Trans. Antennas Propag.*, vol. 57, no. 1, pp. 275–279, Jan. 2009.
- [6] F. Shigeki, "Waveguide line," Jpn. Patent 06-053, 1994.
- [7] J. Hirokawa and M. Ando, "Single-layer feed waveguide consisting of posts for plane TEM wave excitation in parallel plates," *IEEE Trans. Antennas Propag.*, vol. 46, no. 5, pp. 625–630, May 1998.
- [8] M. Bozzi, "Substrate integrated waveguide (SIW): An emerging technology for wireless systems," in *Proc. Asia Pacific Microw. Conf.*, Dec. 2012, pp. 788–790.
- [9] J. P. Quinzant and D. G. Dudley, "Slots in a parallel plate waveguide," *Radio Sci.*, vol. 11, nos. 8–9, pp. 713–724, Aug. 1976.
- [10] T. Keshavamurthy and C. Butler, "Characteristics of a slotted parallel-plate waveguide filled with a truncated dielectric," *IEEE Trans. Antennas Propag.*, vol. AP-29, no. 1, pp. 112–117, Jan. 1981.
- [11] H. A. Auda, "Quasistatic characteristics of the slotted parallel-plate waveguide," *Proc. Inst. Elect. Eng.*, vol. 135, no. 4, pp. 256–262, Aug. 1988.
- [12] Y. Ki Cho, "On the equivalent circuit representation of the slitted parallel-plate waveguide filled with a dielectric," *IEEE Trans. Antennas Propag.*, vol. 37, no. 9, pp. 1193–1200, Sep. 1989.
- [13] Y. Wagatsuma and T. Yoneyama, "Multiply folded sectoral horn fed planar antenna," in *Proc. Commun. Conf. IEICE*, Tokyo, Japan, Sep. 1996, p. 53.
- [14] M. Sato, Y. Konishi, and S. Urasaki, "A traveling-wave fed slot array antenna with inclined linear polarization at 60-GHz band," in *Proc. Commun. Conf. IEICE*, Tokyo, Japan, Sep. 1996, p. 68.
- [15] Y. Wagatsuma, Y. Daicho, and T. Yoneyama, "Leaky NRD-guide fed folded planar antenna," in *Proc. Gen. Conf. IEICE*, Tokyo, Japan, Mar. 1997, p. 177.
- [16] J. Hirokawa, M. Ando, and N. Goto, "Waveguide-fed parallel plate slot array antenna," *IEEE Trans. Antennas Propag.*, vol. 40, no. 2, pp. 218–223, Feb. 1992.
- [17] J. Hirokawa, K. Sakurai, M. Ando, and N. Goto, "An analysis of a waveguide T-junction with an inductive post," *IEEE Trans. Microw. Theory Techn.*, vol. 39, no. 3, pp. 563–566, Mar. 1991.
- [18] S. Germain, D. Deslandes, and K. Wu, "Development of substrate integrated waveguide power dividers," in *Proc. CCECE*, 2003, pp. 1921–1924.
- [19] Z. Hao, W. Hong, H. Li, H. Zhang, and K. Wu, "Multiway broadband substrate integrated waveguide (SIW) power divider," in *Proc. IEEE Antennas Propag. Soc. Int. Symp.*, Jul. 2005, pp. 639–642.
- [20] K. Song, Y. Fan, and X. Zhou, "X-band broadband substrate integrated rectangular waveguide power divider," *Electron. Lett.*, vol. 44, pp. 211–213, Jan. 2008.
- [21] K. Song and Y. Fan, "Broadband traveling-wave power divider based on substrate integrated rectangular waveguide," *Electron. Lett.*, vol. 45, pp. 631–632, Jun. 2009.
- [22] K. Song, Y. Fan, and Y. Zhang, "Radial cavity power divider based on substrate integrated waveguide technology," *Electron. Lett.*, vol. 42, no. 19, pp. 1100–1101, Sep. 2006.
- [23] K. Song, Y. Fan, and Y. Zhang, "Eight-way substrate integrated waveguide power divider with low insertion loss," *IEEE Trans. Microw. Theory Techn.*, vol. 56, no. 6, pp. 1473–1477, Jun. 2008.
- [24] D. S. Eom, J. Byun, and H. Y. Lee, "Multilayer substrate integrated waveguide four-way out-of-phase power divider," *IEEE Trans. Microw. Theory Techn.*, vol. 57, no. 12, pp. 3469–3476, Dec. 2009.
- [25] J. N. Hui, W. J. Feng, and W. Q. Che, "Balun bandpass filter based on multi-layer substrate integrated waveguide power divider," *Electron. Lett.*, vol. 48, pp. 571–573, May 2012.
- [26] D. Wu, Y. Fan, and Z. He, "Vertical transition and power divider using substrate integrated circular cavity," *IEEE Microw. Wireless Compon. Lett.*, vol. 19, no. 6, pp. 371–373, Jun. 2009.
- [27] O. A. Nazarov, V. S. Panko, and Y. P. Salomatov, "SIW unequal Y-type power divider," in *Proc. Int. Siberian Conf. Control Commun. (SIBCON)*, May 2016, pp. 1–3.
- [28] Z. Kordiboroujeni and J. Bornemann, "Efficient design of substrate integrated waveguide power dividers for antenna feed systems," in *Proc. 7th Eur. Conf. Antennas Propag. (EuCAP)*, Gothenburg, Sweden, Apr. 2013, pp. 352–356.

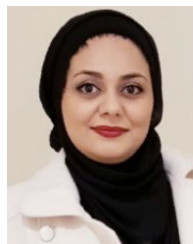
- [29] A. P. Wirawan, P. H. Mukti, and E. Setijadi, "Design of substrate integrated waveguide based power divider for S-band applications," in *Proc. Int. Conf. Radar, Antenna, Microw., Electron. Telecommun. (ICRAMET)*, Bandung, Indonesia, Oct. 2015, pp. 28–31.
- [30] Y. Fu, K. Y. Chan, M. G. Banciu, and R. Ramer, "Broadband Y-type divider in Ku-band using substrate integrated waveguide," in *Proc. Int. Semiconductor Conf. (CAS)*, Oct. 2019, pp. 57–60.
- [31] S. S. Karimabadi and A. R. Attari, "Broadband substrate integrated waveguide four-way power divider," in *Proc. 6th Int. Symp. Telecommun. (IST)*, Nov. 2012, pp. 80–83.
- [32] D. Navarro, L. Carrera, and M. Baquero, "A SIW slot array antenna in Ku band," in *Proc. 4th Eur. Conf. Antennas Propag. (EuCAP)*, 2010, pp. 1–4.
- [33] Z. C. Hao, W. Hong, J. X. Chen, X. P. Chen, and K. Wu, "A novel feeding technique for antipodal linearly tapered slot antenna array," in *IEEE MTT-S Int. Microw. Symp. Dig.*, Jun. 2005, pp. 1641–1643.
- [34] D. Navarro-Méndez, L. Carrera-Suárez, M. Baquero-Escudero, and V. Rodrigo-Peñarocha, "Two layer slot-antenna array in SIW technology," in *Proc. IEEE Eur. Microw. Conf. (EuMC)*, Sep. 2010, pp. 1492–1495.
- [35] A. Suntives and R. Abhari, "Transition structures for 3-D integration of substrate integrated waveguide interconnects," *IEEE Microw. Wireless Compon. Lett.*, vol. 17, no. 10, pp. 697–699, Oct. 2007.
- [36] Y. Zhang, Z. N. Chen, X. Qing, and W. Hong, "Wideband millimeter-wave substrate integrated waveguide slotted narrow-wall fed cavity antennas," *IEEE Trans. Antennas Propag.*, vol. 59, no. 5, pp. 1488–1496, May 2011.
- [37] K. Gong, Z. N. Chen, X. Qing, P. Chen, and W. Hong, "Substrate integrated waveguide cavity-backed wide slot antenna for 60-GHz bands," *IEEE Trans. Antennas Propag.*, vol. 60, no. 12, pp. 6023–6026, Dec. 2012.
- [38] Y. Li and K.-M. Luk, "Low-cost high-gain and broadband substrate-integrated-waveguide-fed patch antenna array for 60-GHz band," *IEEE Trans. Antennas Propag.*, vol. 62, no. 11, pp. 5531–5538, Nov. 2014.
- [39] J. Wu, Y. J. Cheng, and Y. Fan, "60-GHz substrate integrated waveguide fed cavity-backed aperture-coupled microstrip patch antenna arrays," *IEEE Trans. Antennas Propag.*, vol. 63, no. 3, pp. 1075–1085, Mar. 2015.
- [40] H. Jin and G. Wen, "A novel four-way Ka-band spatial power combiner based on HMSIW," *IEEE Microw. Wireless Compon. Lett.*, vol. 18, no. 8, pp. 515–517, Aug. 2008.
- [41] W. Hong, B. Liu, Y. Wang, Q. Lai, H. Tang, X. X. Yin, Y. D. Dong, Y. Zhang, and K. Wu, "Half mode substrate integrated waveguide: A new guided wave structure for microwave and millimeter wave application," in *Proc. Joint 31st Int. Conf. Infr. Millim. Waves 14th Int. Conf. Terahertz Electron.*, Sep. 2006, p. 219.
- [42] B. Liu, W. Hong, L. Tian, H.-B. Zhu, W. Jiang, and K. Wu, "Half mode substrate integrated waveguide (HMSIW) multi-way power divider," in *Proc. Asia-Pacific Microw. Conf.*, Dec. 2006, pp. 917–920.
- [43] D. S. Eom, J. Byun, and H. Y. Lee, "Multilayer four-way out-of-phase power divider for substrate integrated waveguide applications," *IEEE Trans. Microw. Theory Techn.*, vol. 57, no. 12, pp. 3469–3476, Jun. 2009.
- [44] B. Liu, "The application of image transition in HMSIW power splitter design," in *Proc. 4th Int. High-Speed Intell. Commun. Forum*, 2006, pp. 1–2.
- [45] H. F. Talbot, "Facts relating to optical science. No. IV," *Philos. Mag. J. Sci.*, vol. 9, no. 56, pp. 401–407, 1836.
- [46] L. B. Soldano and E. C. M. Pennings, "Optical multi-mode interference devices based on self-imaging: Principles and applications," *J. Lightw. Technol.*, vol. 13, no. 4, pp. 615–627, Apr. 1995.
- [47] T. J. Tayag, M. B. Steer, J. F. Harvey, A. B. Yakovlev, and J. Davis, "Spatial power splitting and combining based on the Talbot effect," *IEEE Microw. Wireless Compon. Lett.*, vol. 12, no. 1, pp. 9–11, Jan. 2002.
- [48] R. Ulrich and T. Kamiya, "Resolution of self-imagings in planar optical waveguides," *J. Opt. Soc. Amer.*, vol. 68, no. 5, pp. 583–592, 1978.
- [49] N. Yang, C. Caloz, and K. Wu, "Substrate integrated waveguide power divider based on multimode interference imaging," in *IEEE MTT-S Int. Microw. Symp. Dig.*, Jun. 2008, pp. 883–886.
- [50] J. F. Xu, W. Hong, P. Chen, and K. Wu, "Design and implementation of low sidelobe substrate integrated waveguide longitudinal slot array antennas," *IET Microw., Antennas Propag.*, vol. 3, no. 5, pp. 790–797, Jul. 2009.
- [51] Y. Cassivi, L. Perregrini, P. Arcioni, M. Bressan, K. Wu, and G. Conciauro, "Dispersion characteristics of substrate integrated rectangular waveguide," *IEEE Microw. Wireless Compon. Lett.*, vol. 12, no. 9, pp. 333–335, Sep. 2002.
- [52] M. D. Pozar, *Microwave Engineering*, 4th ed. Hoboken, NJ, USA: Wiley, 2012.
- [53] Z.-Y. Zhang and K. Wu, "Broadband half-mode substrate integrated waveguide (HMSIW) Wilkinson power divider," in *IEEE MTT-S Int. Microw. Symp. Dig.*, Jun. 2008, pp. 879–882.
- [54] N. A. Smith and R. Abhari, "Compact substrate integrated waveguide Wilkinson power dividers," in *Proc. IEEE Antennas Propag. Soc. Int. Symp.*, Jun. 2009, pp. 1–4.
- [55] K. Kim, J. Byun, and H.-Y. Lee, "Substrate integrated waveguide Wilkinson power divider with improved isolation performance," *Prog. Electromagn. Res. Lett.*, vol. 19, pp. 41–48, 2010.
- [56] T. Djerafi, D. Hammou, K. Wu, and S. O. Tatu, "Ring-shaped substrate integrated waveguide Wilkinson power dividers/combiners," *IEEE Trans. Compon., Packag., Manuf. Technol.*, vol. 4, no. 9, pp. 1461–1469, Sep. 2014.
- [57] A. Moulay and T. Djerafi, "Wilkinson power divider with fixed width substrate-integrated waveguide line and a distributed isolation resistance," *IEEE Microw. Wireless Compon. Lett.*, vol. 28, no. 2, pp. 114–116, Feb. 2018.
- [58] X.-P. Chen, L. Li, and K. Wu, "Multi-antenna system based on substrate integrated waveguide for Ka-band traffic-monitoring radar applications," in *Proc. Eur. Microw. Conf. (EuMC)*, Sep. 2009, pp. 417–420.
- [59] S. Park, Y. Okajima, J. Hirokawa, and M. Ando, "A slotted post-wall waveguide array with interdigital structure for 45° linear and dual polarization," *IEEE Trans. Antennas Propag.*, vol. 53, no. 9, pp. 2865–2871, Sep. 2005.
- [60] M. M. Zhou, Y. J. Cheng, and W. N. Huang, "Substrate integrated slot array antenna with required radiation pattern envelope," *Int. J. Antennas Propag.*, vol. 2016, pp. 1–4, Jan. 2016.
- [61] T. Y. Yang, W. Hong, and Y. Zhang, "Wideband millimeter-wave substrate integrated waveguide cavity-backed rectangular patch antenna," *IEEE Antennas Wireless Propag. Lett.*, vol. 13, pp. 205–208, 2014.
- [62] X. Zou, C.-M. Tong, and D.-W. Yu, "Y-junction power divider based on substrate integrated waveguide," *Electron. Lett.*, vol. 47, no. 25, pp. 1375–1376, 2011.
- [63] M. M. Fahmi, J. A. Ruiz-Cruz, and R. R. Mansour, "Compact ridge waveguide Gysel combiners for high-power applications," *IEEE Trans. Microw. Theory Techn.*, vol. 67, no. 3, pp. 968–977, Mar. 2019.
- [64] H. Chen, X. Wang, W. Che, Y. Zhou, and T. Liu, "Novel Gysel power dividers based on half-mode substrate integrated waveguide (HMSIW)," in *IEEE MTT-S Int. Microw. Symp. Dig.*, Chengdu, China, May 2018, pp. 1–3.
- [65] H. Chen, Y. Zhou, T. Zhang, W. Che, and Q. Xue, "N-way Gysel power divider with arbitrary power-dividing ratio," *IEEE Trans. Microw. Theory Techn.*, vol. 67, no. 2, pp. 659–669, Feb. 2019.
- [66] X. Ren, K. Song, F. Zhang, and B. Hu, "Miniaturized Gysel power divider based on composite right/left-handed transmission lines," *IEEE Microw. Wireless Compon. Lett.*, vol. 25, no. 1, pp. 22–24, Jan. 2015.
- [67] G. Jin, G. Min, and G. Bo, "A novel three-way Gysel power divider/combiner on plane structure," *Prog. Electromagn. Res. Lett.*, vol. 75, pp. 17–113, 2018.
- [68] S. Chen, G. Zhao, and Y. Yu, "A modified Gysel power divider with arbitrary power dividing ratio," *Prog. Electrom. Res. Lett.*, vol. 77, pp. 51–57, 2018.
- [69] F. Lin, Q.-X. Chu, Z. Gong, and Z. Lin, "Compact broadband Gysel power divider with arbitrary power-dividing ratio using microstrip/slotline phase inverter," *IEEE Trans. Microw. Theory Techn.*, vol. 60, no. 5, pp. 1226–1234, May 2012.
- [70] M. J. Park, "Coupled line Gysel power divider for dual-band operation," *Electron. Lett.*, vol. 47, no. 10, pp. 599–600, May 2011.
- [71] Z. Y. Sun, L. J. Zhang, Y. P. Yan, and H. W. Yang, "Design of un-equal dual-band Gysel power divider with arbitrary termination resistance," *IEEE Trans. Microw. Theory Techn.*, vol. 59, no. 8, pp. 1962–1995, Aug. 2012.
- [72] Z. Sun, L. Zhang, Y. Liu, and X. Tong, "Modified Gysel power divider for dual-band applications," *IEEE Microw. Wireless Compon. Lett.*, vol. 21, no. 1, pp. 16–18, Jan. 2011.
- [73] M. Hayati, S. A. Malakooti, M. Jamshidi, and Y. Y. Sarvarani, "A new design of equal and unequal dual-band Gysel power divider with controllable bandwidth," *Electromagnetics*, vol. 33, no. 8, pp. 609–622, Nov. 2013.
- [74] A. Moulay and T. Djerafi, "Gysel power divider with fixed characteristic impedance," in *IEEE MTT-S Int. Microw. Symp. Dig.*, Aug. 2020, pp. 896–899.
- [75] S. Chen, Y. Yu, and M. Tang, "Dual-band Gysel power divider with different power dividing ratios," *IEEE Microw. Wireless Compon. Lett.*, vol. 29, no. 7, pp. 462–464, Jul. 2019.

- [76] R. Nemati, S. Karimian, H. Shahi, N. Masoumi, and S. Safavi-Naeini, "Multisection combined Gysel–Wilkinson power divider with arbitrary power division ratios," *IEEE Trans. Microw. Theory Techn.*, vol. 69, no. 3, pp. 1567–1578, Mar. 2021.
- [77] X. Wang, X.-W. Zhu, C. Yu, P.-F. Liu, and X.-S. Shi, "Design of the quarter-mode substrate integrated waveguide in-phase and out-of-phase filtering power divider," in *IEEE MTT-S Int. Microw. Symp. Dig.*, May 2018, pp. 1–3.
- [78] C. Ma and C. Jin, "Compact triple-mode filter based on quarter-mode substrate integrated waveguide," in *Proc. Asia-Pacific Microw. Conf. (APMC)*, vol. 2, Dec. 2015, pp. 1–15.
- [79] T. R. Jones, M. H. Zarifi, and M. Daneshmand, "Miniaturized quarter-mode substrate integrated cavity resonators for humidity sensing," *IEEE Microw. Wireless. Compon. Lett.*, vol. 27, no. 7, pp. 612–614, Jul. 2017.
- [80] L.-S. Wu, J. Mao, and W.-Y. Yin, "Compact quasi-elliptic bandpass filter based on folded ridge substrate integrated waveguide (FRSIW)," in *Proc. Asia Pacific Microw. Conf.*, Kaohsiung, Taiwan, Dec. 2012, pp. 385–387.
- [81] T. R. Jones and M. Daneshmand, "Miniaturized reconfigurable dual-band bandstop filter with independent stopband control using folded ridged quarter-mode substrate integrated waveguide," in *IEEE MTT-S Int. Microw. Symp. Dig.*, Jun. 2019, pp. 102–105.
- [82] X. Wang, X.-W. Zhu, P.-F. Liu, N.-Y. Zhong, H.-T. Li, and T. H. Le, "Design of the compact eighth-mode substrate integrated waveguide filter with multilayer structure," in *IEEE MTT-S Int. Microw. Symp. Dig.*, May 2019, pp. 1–3.
- [83] Z. Xiangjun, G. Yongxin, and Wangfei, "Minimization of wideband LTCC bandpass filter using QMSIW and EMSIW cavities," in *IEEE MTT-S Int. Microw. Symp. Dig.*, Jul. 2015, pp. 1–2.
- [84] X. Lu and X.-W. Zhu, "Third-order bandpass filter design by EMSIW and QMSIW cavity," in *Proc. Int. Conf. Microw. Millim. Wave Technol. (ICMMT)*, Sep. 2020, pp. 1–3.
- [85] Y. Wang, C. Zhou, K. Zhou, and W. Wu, "A compact filtering power divider based on SIW triangular cavities," in *Proc. IEEE Electr. Design Adv. Packag. Syst. Symp. (EDAPS)*, Dec. 2017, pp. 1–3.
- [86] Y. Liu, E. Wang, H. Zhang, and G. Zhang, "A new two-way multilayer SIW filtering power divider (FPD) with good isolation," in *Proc. Int. Appl. Comput. Electromagn. Soc. Symp.-China (ACES)*, Aug. 2019, pp. 1–2.
- [87] Y.-X. Yan, W. Yu, and J.-X. Chen, "Millimeter-wave low side- and back-lobe SIW filtenna array fed by novel filtering power divider using hybrid TE<sub>101</sub>/TE<sub>301</sub> mode SIW cavities," *IEEE Access*, vol. 9, pp. 167706–167714, 2021.
- [88] H. Chu and Y.-X. Guo, "A filtering dual-polarized antenna subarray targeting for base stations in millimeter-wave 5G wireless communications," *IEEE Trans. Compon., Packag., Manuf. Technol.*, vol. 7, no. 6, pp. 964–973, Jun. 2017.
- [89] H. Chu, J.-X. Chen, S. Luo, and Y.-X. Guo, "A millimeter-wave filtering monopulse antenna array based on substrate integrated waveguide technology," *IEEE Trans. Antennas Propag.*, vol. 64, no. 1, pp. 316–321, Jan. 2016.
- [90] H. Jin, G. Q. Luo, W. Wang, W. Che, and K.-S. Chin, "Integration design of millimeter-wave filtering patch antenna array with SIW four-way anti-phase filtering power divider," *IEEE Access*, vol. 7, pp. 49804–49812, 2019.
- [91] H.-T. Hu and C. H. Chan, "Substrate-integrated-waveguide-fed wideband filtering antenna for millimeter-wave applications," *IEEE Trans. Antennas Propag.*, vol. 69, no. 12, pp. 8125–8135, Dec. 2021.
- [92] J. Zhang, S. Zhang, and G. F. Pedersen, "Dual-band structure reused antenna based on quasi-elliptic bandpass frequency selective surface for 5G application," *IEEE Trans. Antennas Propag.*, vol. 68, no. 11, pp. 7612–7617, Nov. 2020.
- [93] R. Lu, C. Yu, F. Wu, Z. Yu, L. Zhu, J. Zhou, P. Yan, and W. Hong, "SIW cavity-fed filtennas for 5G millimeter-wave applications," *IEEE Trans. Antennas Propag.*, vol. 69, no. 9, pp. 5269–5277, Sep. 2021.



tion, phase shifters, and phased arrays.

**FARAH BILAWAL** (Member, IEEE) received the B.S. degree in electrical engineering from the University of Engineering and Technology (UET), Lahore, Pakistan, in 2012, and the M.S. degree in electrical engineering from the National University of Science and Technology (NUST), Islamabad, Pakistan, in 2016. She is currently pursuing the Ph.D. degree in electrical engineering with Monash University, VIC, Australia. Her research interests include antennas and propaga-



**FATEMEH BABAEIAN** (Member, IEEE) received the doctorate degree from the Department of Electrical and Computer System Engineering (ECSE), Monash University, VIC, Australia, in 2020. She is currently working as a Research Fellow with Monash University. Her research interests include RF, microwave, antenna array synthesis, chipless RFID, biomedical electronics, and signal processing.



His research interests include antennas and propagation, phase shifters, phased array antennas, and mobile networks.

**KIM TUYEN TRINH** (Member, IEEE) received the B.E. degree in telecommunications engineering from Telecommunications University (TCU), Vietnam, in 2002, the M.E. degree in telecommunications engineering from La Trobe University, VIC, Australia, in 2012, and the Ph.D. degree in electrical engineering from Monash University, VIC, Australia, in 2020. He is a Researcher with the Monash Microwave, Antenna, RFID, and Sensor Laboratory (MMARS), Monash University.



with the Department of Electrical and Computer Systems Engineering, Monash University, Melbourne, VIC, Australia. He has authored or coauthored over 220 refereed journals and conference papers, 24 book chapters, and eight books. He holds nine international patent applications on chipless RFID.

**NEMAI CHANDRA KARMAKAR** (Senior Member, IEEE) received the M.Sc. degree in electrical engineering from the University of Saskatchewan, Saskatoon, SK, Canada, in 1991, and the Ph.D. degree from the University of Queensland, Brisbane, QLD, Australia, in 1999. He has over 20 years of teaching, design, and development experience in antennas, microwave active and passive circuits, and RFIDs in Canada, Australia, and Singapore. He is currently an Associate Professor